Genomic architecture of nestmate recognition cues in the desert ant

Pnina Cohen*, Shani Inbar*, Eyal Privman#

Department of Evolutionary and Environmental Biology, Institute of Evolution, University of Haifa, Haifa, Israel

* Equal contribution

Corresponding author: eprivman@univ.haifa.ac.il

Abstract

Nestmate recognition is the basis for cooperation within social insect colonies. Quantitative variation in cuticle hydrocarbons (CHCs) is used for nestmate recognition in ants and other social insects. We carried out a Genome Wide Association Study (GWAS) of CHCs in the desert ant *Cataglyphis niger* by sampling 47 colonies, fully sequencing six workers from each colony, and measuring the relative amounts of their CHCs. Under the Gestalt colony odour model, social interactions between nestmates, in which CHCs are being transferred and mixed, are essential in creating a uniform colony CHC profile. Therefore, we carried out a second GWAS between the colonies and their uniform Gestalt odour by averaging nestmate genotypes and comparing them to their averaged CHC amounts. Our results are in line with the Gestalt model. Together, the two analyses identified 99 candidate QTLs associated with 18 of the CHCs. Thirteen clusters of two to four QTLs located within 10cM from each other were identified, seven of which contained QTLs from both analyses. We conclude that nestmate recognition cues are a complex quantitative colony-level trait with a significant genetic component to their phenotypic variation and a highly polygenic architecture.

Introduction

Colonial identity is the foundation and a prerequisite for any social interaction in insect societies. The ability to recognize nestmates and to discriminate them from aliens is needed for protecting the colony's food reserves and brood from being plundered and for preserving territorial control over resources around the nest. In most social insect species, nestmates have high genetic relatedness, in keeps with Hamilton's principles of kin selection and inclusive fitness[1,2], and nestmate recognition is equivalent to kin recognition. A major class of chemical cues that facilitate nestmate recognition are lipids found on the cuticle, mainly n-alkanes, methyl-branched, and unsaturated hydrocarbons[3–8]. Insect cuticular hydrocarbons (CHCs) chains vary in length (up to 60, but mostly between 20 and 40 carbons), number and positions of methyl branches, and number and positions of double bonds[9]. Social insect species generally display relatively large numbers of different CHCs[10]. While different insect species have qualitatively distinct mixtures of CHCs, intraspecific variation of CHC mixtures is chiefly quantitative. The relative amounts of CHCs are the chemical profile that make up its identity[11–13]. In ants, the numbers of different CHCs are especially large, even in comparison to other social insects[10], with dozens of distinct CHCs on the body surface of a single individual.

Intra-colony CHC composition variability is smaller than inter-colony variability[6,14], and some studies reported that chemical distances (dissimilarity) between CHC profiles of colonies correlate with aggression levels between members of these colonies[15–17]. Diet, nest material, and other environmental factors were shown to influence ant CHC

47 profiles[18–20] and thereby contribute to nestmate recognition and inter-colony aggression.
48 Evidence from various studies indicates that genetic factors are also important
49 contributors to the colony-specific composition of CHCs (reviewed by Sprenger and
50 Florian[21]). Correlation between genetic and chemical distances was reported for the
51 yellow crazy ant[15], the Argentine ant[17], and the clonal raider ant[22]. Provost[23] conducted
52 controlled crosses of *Leptothorax lichtensteini* to produce unfamiliar ants with varying
53 degrees of genetic relatedness, demonstrating aggression is correlated with genetic
54 distance. A genetic component to nestmate recognition is also supported by cross-
55 fostering experiments in *Formica rufinarbis*[24]. While these studies provided support for
56 the hypothesis that CHCs are affected by genetic polymorphism, so far no study has
57 identified specific genomic loci that may be responsible for such genetic effects.

58 Two models were suggested for the mechanism that creates a colony specific CHC
59 profile[25]. In the individualistic model, all CHCs found on an individual are self-produced.
60 Under this model, the similarities between nestmate CHC profiles may be explained by
61 shared genetics between the closely related colony members and by their shared
62 environment. The alternative model is that of the colony Gestalt odour, in which CHCs
63 are transferred and mixed between colony members via allogrooming and/or
64 trophallaxis (transfer of food)[5,24,26–28] . This serves to reduce intra-colony variability,
65 which may prevent nepotism in colonies with some kin structure (e.g. in patrilines of a
66 monogyne, polyandrous colony). These two alternative hypotheses were examined in
67 multiple studies, some of which support either of the two models. For example, when
68 colonies of *Cataglyphis Iberia* ants were divided into two groups their CHC profiles
69 diverged and inter-group aggression transpired[29]. The CHC profiles converged after the

separated groups were reunited, as expected under the Gestalt model. In another study, on *Rhytidoponera confuse* ants, levels of aggression towards nestmates were measured after members of two colonies were caged together[30]. This study concluded that the individualistic component is a greater contributor to the colony chemical identity than the homogenizing Gestalt effect.

The uniform CHC profile of a colony is a colony-level phenotype, a phenotype which is the combined output (the average or any other function) of the individual phenotypes of nestmates. As with any other phenotype, colony-level phenotypes may be affected by internal factors such as genetics, epigenetics, animal size, and its health, and external factors such as nest material, diet, predation pressure, weather, and seasonality. Other examples of colony-level phenotypes in social insects include alternative social structures, such as the monogyne versus polygyne social structures in fire ants[31], collective activities such as foraging and nest construction[32,33], and social immunity, the defensive actions taken against pathogens and parasites[33–35]. In ants and other eusocial insects, a colony is typically made of close relatives that may be regarded as a single colonial organism or a superorganism[36,37]. Therefore, it is useful to consider a colony-level genotype as a high-ploidy genotype of a single entity. These collective genotypes may be studied for their association with any collective colony phenotype, in our case, the homogenized CHC profiles.

Here, we carried out the first Genome Wide Association Study (GWAS) to search for the genetic basis of among-colony variation in CHCs. Based on a pilot study on the power of alternative approaches for executing a colony-level GWAS[38], we sampled 47 colonies of

92 the ant *Cataglyphis niger* and fully sequenced the genomes of six workers from each
93 colony. We tested for association between genomic polymorphism and the quantities of
94 34 CHCs using two approaches. The first was a standard GWAS of individual genotypes
95 and phenotypes. We then conducted a colony-level GWAS, motivated by the Gestalt
96 model. In the second analysis, we tested for associations between the colony-level
97 genotypes, represented by the colonial allele frequency in each locus, and colony-level
98 (averaged) CHC profiles. These analyses revealed candidate loci that underlie inter-
99 colony variation in CHC profiles, which constitute the genomic basis for nestmate
100 recognition cues.

101 Materials and methods

102 Study population

103 This study used a population sample from Betzet beach on the northern Israeli
104 coastline. This population was previously referred to as *Cataglyphis drusus*[39], but our
105 recent species delimitation study suggested that this is the same species as *C. niger*,
106 because these populations are not differentiated by their nuclear genomic DNA[40]. We
107 note that some populations of *C. niger* include polygyne colonies (headed by multiple
108 egg-laying queens)[40] and that our recent study revealed that this social polymorphism is
109 associated with a supergene (Lajmi *et al.* in prep). However, the study population used
110 here is purely monogyne (each colony is headed by a single queen)[39,40]. The supergene
111 is always homozygous (MM) in monogyne samples (and always heterozygous MP in
112 polygyne samples), so we do not expect it to affect the population genetics and the
113 performance of GWAS in this study population. *C. niger* queens are mated with 2-9

114 males (polyandrous), resulting in an average of 0.26 within-colony genetic
115 relatedness[39,40].

116 **Sampling scheme**

117 We collected ants from nests dug along a 4 km transect in Betzet beach (from to
118 N33.07868, E35.10705 to N33.05162, E35.10245; Figure 1) between April 24 and May
119 10, 2016. At least 30 workers were sampled from each of 50 nests, 47 of which were
120 used in this study (N35.10297, E33.05339 - N33.05162, E35.10245). The other three
121 nests were used in the pilot stage of this GWAS[38].

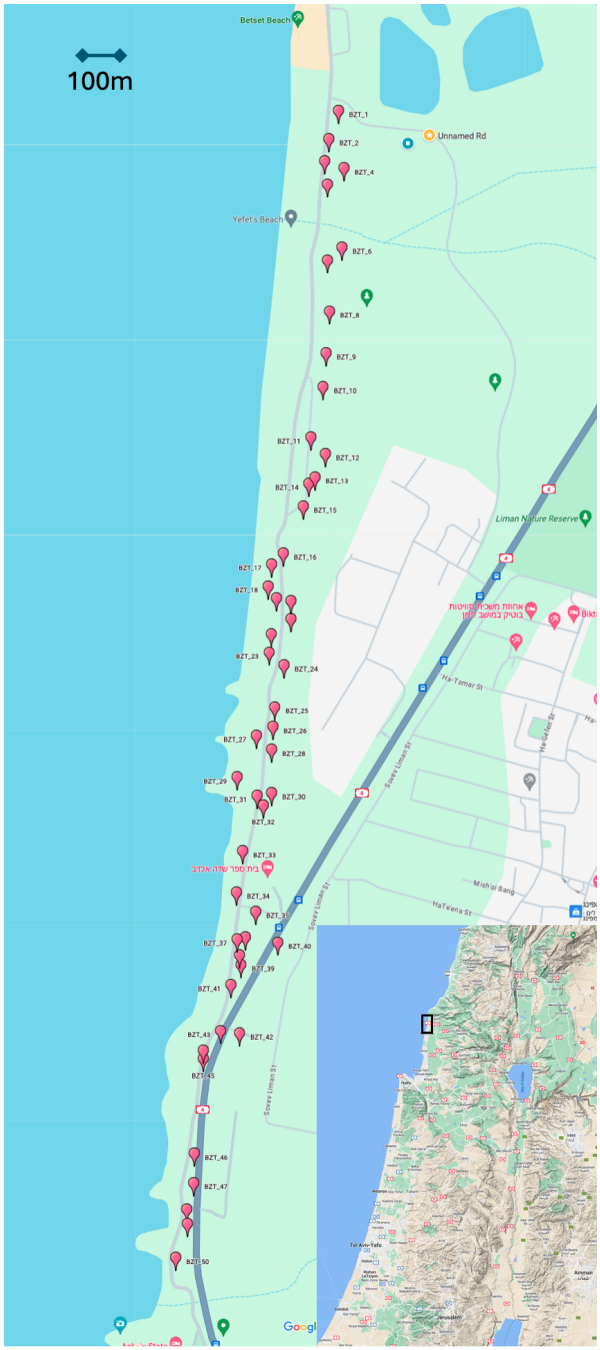

Figure 1. Map of 50 sampled nests along a transact in Betzet Beach in northern Israel (from to N33.07868 E35.10705 to N33.05162 E35.10245).

Behavioural assays

There exists extensive literature on nestmate recognition studies in *C. niger* showing that CHCs are a major component of the chemical cues that workers use to discriminate non-nestmates from nestmates[6,28]. Behavioural assays were previously conducted in our

129 study population, demonstrating that workers from different colonies discriminate
130 nestmates from non-nestmates even between nests that are only 100m apart[40]. We
131 conducted dyadic aggression assays to compare encounters between nestmates and
132 between non-nestmates. The results confirm that the nests we sampled indeed exhibit
133 the ability for nestmate recognition. See Inbar and Privman[41] for the details of this
134 behavioural assay.

135 **Pilot study, experimental design, and power analysis**

136 Before sequencing and analysing our GWAS samples we conducted a pilot study to
137 determine which experimental design gives maximal statistical power to detect QTLs for
138 colony-level traits. In this pilot, we compared different combinations of population
139 genomic methodologies and approaches, and also used to empirical results as a basis
140 for a simulation study to assess statistical power. Please see the full details in Inbar *et*
141 *al.*[38]. Based on the conclusions from this study we chose to conduct whole genome
142 sequencing on six individual samples per colony. Naturally, the more samples the better,
143 but the simulations showed diminishing returns for increasing the number of samples
144 per colony. We note that this is true even though our study population consists of
145 multiply mated queens (we simulated up to ten matings per queen, in line with
146 estimates of 2-9 patrilines per colony in *C. niger*[40]). Based on these results we expect
147 our GWAS to have 37% and 64% probability to detect QTLs that explain 23% and 52%
148 of the variation in the studied trait, respectively (with a *p*-value of 5% after correction
149 for multiple testing).

150 **Whole genome sequencing**

151 For six individuals from each of the 47 nests, DNA was extracted from the head and
152 abdomen (QIAGEN AllPrep DNA/RNA Mini kit) and the thorax was used for the chemical
153 analysis of CHCs (see below). A uniquely barcoded genomic library was constructed for
154 each sample following the standard protocol of the Illumina TruSeq Nano DNA Library
155 Prep kit. Briefly, a Covaris S220 sonicator was used for DNA shearing aiming for 550bp
156 inserts, ends were repaired, and the fragments were size-selected and purified using
157 magnetic beads (supplied in kit). Then, an adenosine was added to the 3' end of the
158 blunt fragments, individually barcoded adaptors were ligated, and ligated fragments
159 were amplified (eight PCR cycles). Libraries were pooled at equal quantities as three
160 separate pools, each of which was sequenced in two lanes of a paired-end, 150bp
161 reads, on a HiSeq X Ten Illumina sequencer (six lanes in total).

162 **Sequence data processing and genotype calling**

163 *Raw reads pre-processing*

164 Whole-genome sequence data were successfully obtained for 276 of the 282 samples
165 (four from colony 10, five from colonies 18, 19, 22 and 29 and six from each of the
166 other colonies). A total of 5,941,275,998 reads of 150bp were sequenced, with an
167 average of 21,526,362 reads per sample, which is an average genome coverage of 12X
168 (0.5X – 28X). Duplicate read pairs were removed and low quality reads and adaptor
169 contaminations were trimmed or removed using Trimmomatic[42] version 0.36, leaving
170 sequences that were at least 75bp long. The total number of remaining reads was
171 5,527,107,050 (93% of the raw data). Reads were aligned to the *C. niger* reference
172 genome (version Cnig_gn2) using Bowtie2[43] version 2.2.5 run with the 'very-sensitive'

173 and 'end-to-end' settings. 3,216,552,155 reads (54% of raw reads) remained after the
174 filtering out alignments with three or more mismatches or multiple mapping, which were
175 defined as reads with a second best match that has less than twice the number of
176 mismatches as the best match. HaplotypeCaller of the Genome Analysis Toolkit (GATK)
177 package[44] version 3.7 was used to create a Single Nucleotide Polymorphism (SNP)
178 catalogue containing 2,792,460 SNPs.

179 In a first stage of filtering, we removed indels and SNPs with more than two alleles from
180 the catalogue, leaving 2,413,918 SNPs. 16 samples (all four of colony 10, three of
181 colony 11, two of colony 9 and one of colonies 2, 8, 15, 16, 25, 40 and 42) were
182 removed because they were missing genotype data in more than 50% of the loci,
183 leaving 260 individuals from 46 colonies in the analysis.

184 *SNPs catalogue for GWAS*

185 In a second stage of filtering we required for each locus to have genotype calls for at
186 least 80% of the samples with a minimum number of 6 reads per genotype call, a
187 maximum of 250, and a minimum minor allele frequency (MAF) of 15%. In order to
188 remove false SNPs that are the result of collapsed repetitive sequences in the reference
189 genome assembly, a control for these was made using three haploid male *C. niger*
190 sampled in Betzet Beach (33°4'40.88"N/35°6'33.97"E) that were fully-sequenced with
191 high coverage (177X, 55X and 72X). This was done by creating a blacklist of loci where
192 one or more of these haploid samples appears to be heterozygous, which indicates an
193 artifact because male ants are haploid. All SNPs within 600 bp of such heterozygous loci
194 were removed from the catalogue. Additionally, excessively covered SNPs, defined as
195 loci with an average number of reads per sample > 20 (average genome coverage + 2 x

196 standard deviation – see Supplementary Figure S1A). We then removed 14 samples that
197 had more than 60% missing genotypes after this filtering, and as a result had to
198 exclude colony 9 because it had only two samples left. We were left with 244 individuals
199 from 45 colonies (three from colony 11 and 29, four from colony 7, 8, 25 and 32, five
200 from colonies 2, 14, 15, 16, 18, 19, 20, 22, 26, 30, 40 and 42 and six from all the rest)
201 and 171,570 SNPs. The average coverage of this filtered SNP catalogue across the
202 remaining 244 individuals was 10.2X (calculated by the actual number of reads covering
203 the SNPs). Overall, 6,348,274 (15.2%) of all possible 41,863,080 locus X sample
204 combinations did not have genotype call (missing data).

205 *Colonial genotype processing and calculation*

206 For the colony-level analysis, we required that every locus had genotype calls in at least
207 three individuals in each colony, further reducing the number of SNPs to 171,355.
208 Overall, 659,721 (8.6%) of possible 7,710,975 locus X colony combinations did not have
209 genotype call (missing data). We defined colony-level genotypes as the estimated allele
210 frequency of the colony at every locus, which essentially means that a colony is treated
211 as a single polyploid organism. For example, if the genotypes of six members of a
212 colony are 00, 01, 01, 11, 11, 11, where 0 and 1 represent the two alternative alleles in
213 a locus, their individual genotypes were coded in the input file for the GWAS analysis as
214 0, 1, 1, 2, 2, 2 and their colony-level genotype was calculated as an average:
215 $\frac{(0+1+1+2+2+2)}{6} = 1\frac{1}{3}$.

Kinship inference

Individual-level kinship based on the whole-genome data

To create the kinship matrix on the individual level, we chose stringent filtering criteria to ensure low missing data rates and allowed low frequency alleles, which provide useful information for inference of identity-by-descent (IBD) of haplotypes. We filtered the SNP catalogue of the whole-genome sequenced samples (after first stage filtering) so that each locus had genotype calls in at least 88% of the samples with a minimum of 6 reads, a maximum of 250, and a minimum MAF of 1%. Here the MAF cutoff was reduced relative to the GWAS analysis above because rare alleles are a powerful signal for kinship. A MAF of 1% still requires a minimum of two samples that share the minor allele (if homozygous; more if heterozygous), which makes it unlikely to be an artifact due to sequencing errors. We controlled for and filtered out reads that were mapped to suspected collapsed repetitive sequences in the reference as described above, and similarly removed 16 samples from the analysis due to insufficient genotype calls. This resulted in a catalogue of 88,238 SNPs. Using the program Beagle[45], we imputed and phased the catalogue to the total of 9,634 phased segments. The refined-IBD algorithm[46] was used to identify shared haplotypes between the samples. A kinship matrix was created based on the total length of IBD haplotypes shared between every pair of samples.

Colony-level kinship based on RAD-sequencing

To better estimate kinship between colonies, one individual from each of the 47 colonies was chosen to be sequenced with greater sequencing depth using a reduced-representation genomic sequencing approach: the double-digest Restriction-site

239 Associated DNA sequencing (ddRAD-seq) protocol. The rationale for this is that kinship
240 inference by detection of haplotypes that are identical by descent (IBD) between pairs
241 of samples depends on low genotype error rates. Using ddRAD-seq we could sequence a
242 smaller number of loci to a much greater depth (65X – see below), which reduces the
243 genotype error rate.

244 *Restriction-site associated DNA (RAD) sequencing*

245 For one worker per nest, a library was constructed according to a ddRAD-seq protocol
246 based on protocols from Peterson *et al.*[47] and Brelsford *et al.*[48]. Briefly, DNA was
247 digested by two different restriction enzymes (EcoRI as the rare-cutter; MseI as the
248 frequent-cutter) and ligated to barcoded adaptors for multiplexing. Products were
249 amplified using Q5 Hot Start Polymerase (NEB), with the number of cycles reduced to
250 20, the number of replicates increased to four, and starting DNA volume increased to
251 6ul. Also, primers and dNTPs were added to the final thermal cycle in order to minimize
252 single-stranded or heteroduplex PCR products. The libraries were sequenced in one lane
253 of a paired-end, 150bp reads, on a HiSeq X Ten Illumina sequencer.

254 *Pre-processing of RAD-seq data*

255 A total of 823,087,220 reads were sequenced from 47 workers (one from each of the
256 colonies), which is an average expected depth of 65X (14X – 105X) based on the
257 number of restriction sites in the reference genome. The raw reads were initially
258 processed using the *Stacks* pipeline[49] version 2.2. Low quality reads were discarded if
259 their quality score dropped below an averaged phred score of 10 in a sliding window of
260 15% of the reads' length. After this initial processing, 736,899,655 reads that were

261 assigned to a sample remain (90% of raw data). The reads were mapped to the
262 reference genome of *C. niger* (version Cnig_gn2) using *Bowtie2* and filtered using the
263 same criteria as for the whole-genome data above. After this filtering, 718,157,408
264 alignments remained. We continued to analyse the mapped sequences using the *gstacks*
265 program of the *Stacks* pipeline and created a catalogue containing 90,006 SNPs for the
266 47 samples.

267 *Combining the catalogue with additional samples from across Israel*

268 To increase the number of samples and thereby improve SNP calling, imputation and
269 phasing, we made use of another data set that included 103 RAD-sequenced *C. niger*
270 and *C. israelensis* individuals sampled across Israel (described in Rainer-Brodetzki *et*
271 *al.*[40]). The combined catalogue that was created from the 150 individuals contained
272 346,940 SNPs.

273 The following filtering parameters were used: each locus was required to have a
274 genotype call in at least 90% of the samples, with the minimal number of reads of 3, a
275 maximum of 4000, and had a minimum MAF of 1.5%. We controlled for collapsed
276 repetitive elements by using the blacklist described above and by removing excessively
277 covered SNPs, which were defined as loci with a mean number of reads > 250 (mean
278 coverage + 2 x standard deviation – see Supplementary Figure S1B). After filtering,
279 21,179 polymorphic sites remained in the combined catalogue.

280 *Colony-level kinship inference based on RAD-seq data*

281 As with the whole-genome data, the RAD-seq SNP catalogue was imputed and phased
282 using Beagle and refined-IBD to a total of 502 phased segments across the genome.

283 Shared IBD haplotypes between individuals were identified and a kinship matrix was
284 created based on the total length of IBD haplotypes shared between every pair of
285 samples representing 47 colonies.

286 **Chemical analysis of cuticular hydrocarbons**

287 *Cuticular hydrocarbon (CHC) analysis*

288 CHCs were measured for the same six workers from each of the 47 nests that were
289 used for genomic sequencing. Thoraces were individually immersed in hexane to extract
290 non-polar cuticular lipids from each sample separately. Initial analysis was conducted by
291 gas chromatography/mass spectrometry (GC/MS), using a VF-5ms capillary column,
292 temperature-programmed from 60◦C to 300◦C (with 1 min initial hold) at a rate of 10◦C
293 per min, with a final hold of 15 min. Compounds were identified according to their
294 fragmentation pattern and respective retention time compared to authentic standards.
295 Subsequently, all samples were assayed quantitatively by flame ionization gas
296 chromatography (GC/FID), using the above running conditions. Peak integration was
297 performed using the program Varian Galaxie (version 1.9) and relative amounts of each
298 compound were calculated. The relative amounts of each CHC were calculated for each
299 sample. We confirmed that different nests have distinct CHC profiles using a linear
300 discriminant analysis (LDA p-value<0.0001; Supplementary figure S2). For the colony-
301 level analysis, the relative amounts were averaged between the members of each
302 colony.

303 *Normalization of the CHC relative amounts*

304 Outliers to the distribution of each CHC in each of the two datasets (individual relative
305 amounts and averaged colony relative amounts) were removed. These were defined as
306 the amounts that were 1.5 times higher or 1.5 times lower than the interquartile range
307 (the difference between the 75th and 25th percentiles of the distribution). For each
308 dataset, we normalized the distribution of the remaining values using the R package
309 *bestNormalize*[50], which chooses the best fitting normalization function for the dataset on
310 the basis of the Pearson's P statistic. See Supplementary Table S1 for more details.

311 **CHC GWAS**

312 In order to test for a genetic basis of variation in CHCs, we conducted a Genome Wide
313 Association Study (GWAS) over the relative amounts of each CHC, in two levels. The
314 first is the individual level, in which we used the catalogue of genotypes created for the
315 244 samples in 45 colonies, as described above, and their relative amounts of CHC. The
316 second level is the colony level, in which we used the catalogue of colony-level
317 genotypes created for the 45 colonies, as described above, and their averaged colony-
318 level CHC relative amounts.

319 The standard practice for GWAS is the use of a Mixed Linear Model (MLM), in which the
320 population structure and the genetic variation are represented as fixed effects, and
321 kinship between samples as random effects. Here, for each dataset (individual or colony
322 level), we to accounted for sample relatedness by the respective kinship matrix (whole-
323 genome or RAD sequencing data for the individual- or colony-level datasets,
324 respectively) and for population structure by a Principle Component Analysis (PCA) of
325 the SNPs over 45 dimensions in the individual-level analysis and 8 dimensions in the

326 colony-level analysis. The number of dimensions was chosen based on the fit of
327 quantile-quantile (Q-Q) plots – see below.

328 *Execution of GAPIT*

329 Genomic Association and Prediction Integrated Tool (GAPIT)[51] is an R package which
330 executes the Efficient Mixed Model Association (EMMA)[52] method, a computationally
331 efficient algorithm for the study of genomic association using MLM. We ran the program
332 for each CHC in each dataset separately using the Multiple Loci Mixed Linear Model
333 (MLMM), which is implemented in GAPIT by a forward-backward stepwise MLM
334 regression. In each step, the loci that were found to be significantly associated with the
335 trait in the former step are added to the model as cofactors. Accounting for the effect of
336 multiple loci on the trait reduces residual variation in the trait and allows for a greater
337 statistical power in QTL detection. We evaluated how well the model accounts for
338 population structure and kinship using Q-Q plots: plotting the negative logarithm of the
339 assessed *p*-values and comparing them to the expected distribution of *p*-values under
340 the null hypothesis of no association, as calculated by GAPIT. See Supplementary Figure
341 S3. Of the 171,570 / 171,355 loci analysed, 155,815 / 155,807 were mapped to a
342 linkage group on the genetic map[52].

343 *Empirical permutation test*

344 To account for additional unknown confounding factors and other potential problems in
345 the model that might lead to false inference of association, we performed a permutation
346 test to empirically calculate a null distribution of *p*-values when no association between
347 the genotype and phenotype exists: for each CHC, we randomly shuffled the trait values

348 between the samples. Using the shuffled traits and leaving the other model parameters
349 unchanged, we rerun GAPIT 100 times. We did this for both the individual-level and
350 colony-level analyses. For each trait, the original *p*-values of the original run were re-
351 evaluated by comparing them to the distribution of the *p*-values in the shuffled datasets.
352 The *p*-values were further corrected for multiple testing using the Benjamini-Hochberg
353 false discovery rate (FDR) method[53]. We report associations above multiple significance
354 thresholds, with FDR ranging from 5% to 30%. While it is not common to report results
355 with 30% FDR, we find it useful to include this lower threshold. For example, in the
356 individual-level GWAS we report 69 loci above this threshold. While 30% of them are
357 expected to be false positives, these results show that approximately 48 loci (70%) are
358 associated with CHCs across the genome. We ask our readers to keep this in mind while
359 considering our results.

360 Results

361 We conducted a GWAS to identify the genetic basis of variation in CHCs. We tested for
362 associations between the relative amounts of 34 CHCs and genotype calls at 171,570
363 SNPs identified through the whole-genome sequencing of 244 workers from 45 colonies
364 of *C. niger* (3 – 6 ants from each colony). As part of the analysis, relatedness between
365 samples is accounted for by a kinship matrix and population structure is accounted for
366 using a PCA. This analysis was conducted both at the individual level and at the colony
367 level, where the colony phenotype was defined as the averaged CHC level in the colony
368 and the colony genotype as the allele frequency in the colony. Each locus was assigned
369 with a *p*-value for its association with each of the traits, which we corrected for multiple
370 testing into *q*-values.

371 **Population structure and kinship between colonies**

372 It is important to account for population structure and kinship between samples before
373 conducting a GWAS. We analysed population structure using principle component
374 analysis (PCA) of RAD-seq data from one sample of each of the 47 colonies. This
375 analysis revealed limited spatial variation along the north-south axis (Supplementary
376 Figure S4). This may be due to limited dispersal during mating flights. Kinship among
377 samples was inferred from the whole-genome sequencing data based on the total
378 length of shared IBD haplotypes (Supplementary Figure S5A). As expected, and with
379 very few exceptions, stronger kinship was identified between sample collected from the
380 same nest (intra-colony kinship) relative to kinship between nests (inter-colony kinship).
381 The inter-colony kinship between members of colonies 33 and 47 was found to be
382 similar to intra-colony kinship. A possible explanation is that the queens of these two
383 colonies were closely related, either a mother and a daughter (50% related) or full
384 sisters (75% related). There is also high relatedness between some members of
385 colonies 40, 41 and 42. And there appears to be some kinship among colonies 1 – 20
386 (northern part of the transect) and among colonies 32 – 47, in line with the limited
387 structure observed in the PCA results. Kinship was also inferred from more deeply
388 sequenced RAD-seq data from one representative of each colony. High sequencing
389 depth is expected to give lower genotype error rate, which is important for kinship
390 inference. Various levels of inter-colony kinship were observed, mostly between
391 neighbouring nests, which also supports the hypothesis of short range dispersal
392 (between colonies 16 and 19; colonies 34 and 37; colonies 35, 40, 41 and 42; and
393 colonies 46 and 47; see Supplementary Figure S5B).

394 **Individual-level GWAS**

395 The individual-level GWAS identified 13 QTLs that were found to be associated with one
396 of the CHC with the corrected *q*-value < 0.1, three of which were mapped to genes
397 (Figure 2 and Table 1). Two of the QTLs found associated with 5Me-C25 were only
398 4.6cM apart of on chromosome 15. Additionally, 3, 13, 39, and 69 loci were found to be
399 associated with one of the traits with a *q*-value < 5%, 10%, 20%, and 30%,
400 respectively. Of these, 22 were located within a gene or within 2000 bp upstream from
401 a gene's start codon (gene hits). We note that for the lower significance threshold 30%
402 of the associations are expected to be false positives, so approximately 48 out of 69
403 putative QTLs are expected to be true positives. We also used Q-Q plots to assess the
404 distribution of *p*-values under the null hypothesis of no association. These plots show
405 that the association test was well-controlled for potential artefacts such as kinship or
406 non-normal trait distributions that might result in false positives (Supplementary Figure
407 S3).

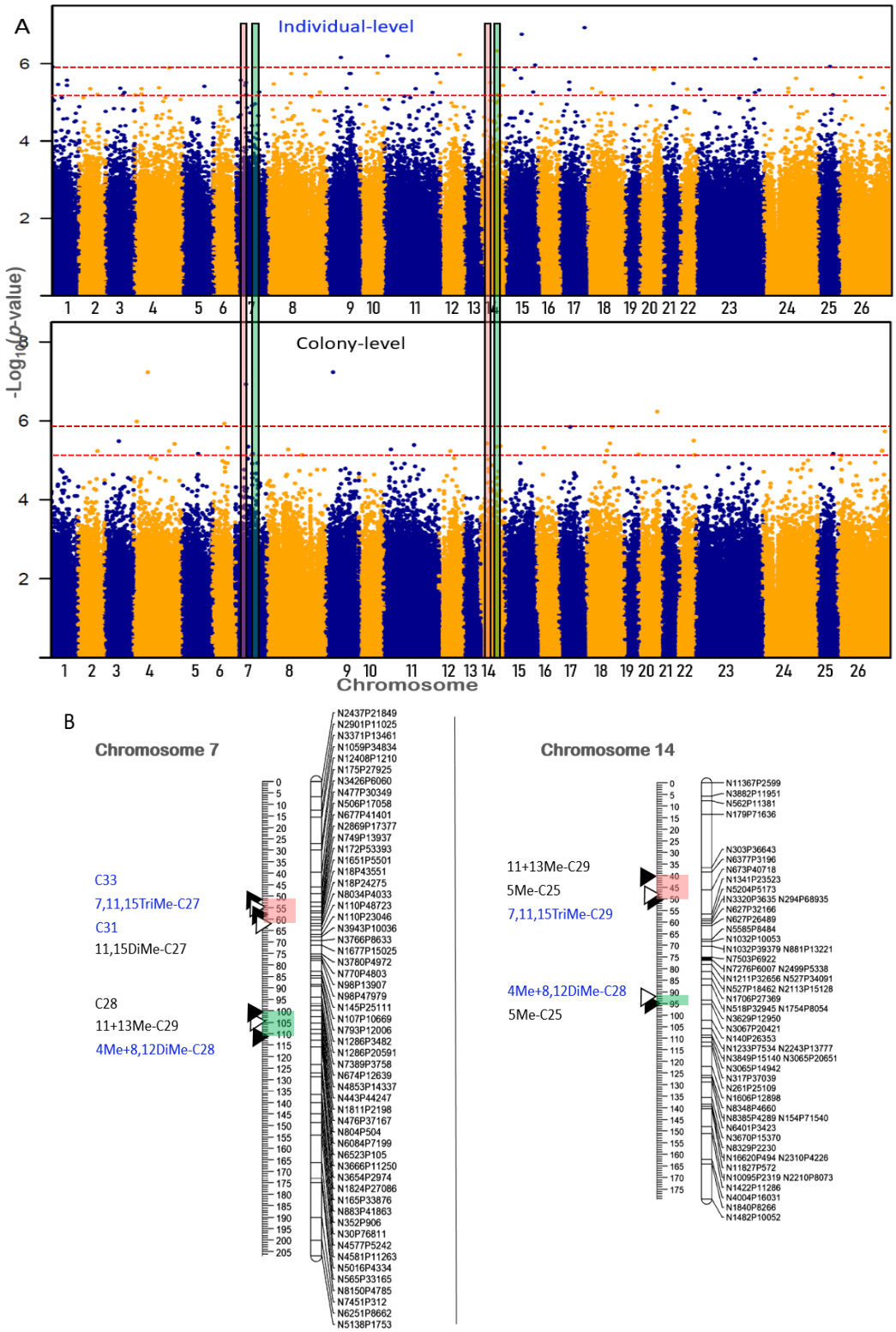

408 **Figure 2. Manhattan plots of associations between loci and CHCs** from the individual-
409 level (A) and colony-level (B) GWAS. Loci above the maroon dotted line are statistically
410 significant with false discovery rate (FDR) of 10%. Loci above the red dotted line are statistically
411 significant with FDR of 30%. Four QTL clusters with QTLs identified in the individual-level and in
412 the colony-level analyses are marked on chromosomes 7 and 14 and presented in detail (B).
413 The associated CHCs are shown in the order of their appearance on the chromosome
414 (individual-level QTLs in blue and colony-level QTLs in black)

415 **Table 1**. Candidate loci and genes that were found to be associated with CHCs in the individual-
416 level GWAS

CHC	*q*-value threshold				Genes (*q*-value)
	0.05	0.1	0.2	0.3	
3Me-C25	-	-	-	4	Discoidin domain-containing receptor 2 (0.282)
5Me-C25	2	4	7	7	Sodium-coupled monocarboxylate transporter 1 (0.106)
					Protein Wnt-10a (0.106)
					2-oxoglutarate and iron-dependent oxygenase domain-containing protein 3 (0.093)
					MIP18 family protein galla-1 (0.093)
4,12DiMe-C26	-	-	2	5	Putative sperm flagellar membrane protein (0.280)
11+13Me-C27	-	-	1	1	Putative protein (0.173)
7,11,15TriMe-C27	1	1	4	8	DDB1- and CUL4-associated factor 5 (0.018)
					Troponin I (0.265)
12Me-C28	-	3	3	5	Follistatin (0.094)
4Me+8,12DiMe-C28	-	1	4	10	Pyridoxal-dependent decarboxylase domain-containing protein 1 (0.211)
					39S ribosomal protein L12, mitochondrial (0.211)
					Putative protein (0.211)
					Putative protein (0.168)
C29	-	-	2	5	Protein phosphatase Slingshot homolog 1 (0.285)
7,11,15TriMe-C29	-	-	-	3	Putative protein (0.254)
2Me-C30	-	-	1	4	
4Me-C30	-	1	1	1	
C31	-	-	8	9	Cadherin-99C (0.144)
					Kinesin-like protein KIF6 (0.144)
					Putative protein (0.144)
					Putative protein (0.226)
C32	-	3	5	5	Putative protein (0.091)
C33	-	-	-	2	Domain of unknown function (0.282)
All	3	13	39	69	

417 **Colony-level GWAS**

418 The colony-level GWAS identified three QTLs that were found to be associated with 5Me-
419 C25, two of which with *q*-value < 0.05 (Figure 2 and Table 2). These QTLs were located
420 on different chromosomes from the loci identified in the individuals-level analysis. Two
421 additional QTLs were found to be associated with two other CHCs. There are 4, 5, 16,
422 and 30 QTLs that with a *q*-value < 5%, 10%, 20%, and 30% that were found to be
423 associated with CHCs, of these, six were gene hits. We note that for the lowest

424 significance threshold 30% of the associations are expected to be false positives, so
425 approximately 21 out of 30 putative QTLs are expected to be true positives.

426 **Table 2**. Candidate loci and genes that were found to be associated with CHCs in the colony-
427 level GWAS.

CHC	*q*-value threshold				Genes (*q*-value)
	0.05	0.1	0.2	0.3	
5Me-C25	2	3	6	7	Sterile alpha and TIR motif-containing protein 1 (0.142)
11+13Me-C27	1	1	1	3	Aminopeptidase N (0.276)
11,15DiMe-C27	1	1	1	4	Protein TANC2 (0.298)
C28	-	-	-	7	Progestin and adipoQ receptor family member 4 (0.227)
					Protein gooseberry-neuro (0.261)
11+13Me-C29	-	-	7	8	Claudin tight junction (0.233)
3Me-C29	-	-	1	1	
All	4	5	16	30	

428 Put together, 99 QTLs were found to be associated with CHCs with *q*-value < 0.3. The
429 QTLs distribution across the genome was found to be significantly different than a
430 uniform distribution in a Kolmogorov-Smirnov test (D = 5038.9, *p*-value < 2.2×10^{-16}).
431 We identified 13 clusters of two to four loci that were within 10cM long from each other.
432 Seven of the clusters included QTLs from both individual- and colony-level analyses
433 (Supplementary Table S2). Overall, 32 of the 99 QTLs were in clusters. There were
434 additional three clusters, each containing 2 QTLs that were more than 10cM but less
435 than 12cM from each other.

436 Of the gene hits, some are implicated in metabolism of amino acids. For example,
437 pyridoxal-dependent decarboxylase domain-containing protein 1 contains a QTL for
438 4Me+8,12DiMe-C28. Other QTL genes are regulatory factors such as protein
439 phosphatase Slingshot homolog 1 for C29. Other genes code for claudin, cadherin and
440 kinesin, which may affect cell structures and functions.

441 ## Discussion

442 We conducted a GWAS of CHC profiles in the desert ant *C. niger* on both the individual
443 and the colony level. We detected a total of 99 loci associated with CHCs across the
444 genome. These results show that the genomic architecture of nestmate recognition cues
445 is highly polygenic. We found one or more putative QTLs for 18 of the 34 CHCs (q-value
446 < 0.3): 14 in the individual-level analysis and 6 in the colony-level analysis. Two CHCs
447 appeared in the results of both analyses (5Me-C25 and 11+13Me-C27). For the
448 remaining 16 CHCs, either their QTLs were missed due to problems in the analysis itself,
449 such as chemical measurement or sequencing errors, wrong model choice, inaccurate
450 kinship inference, etc., or because the contribution of genetics to their quantitative
451 variations was too low to be detected with limited statistical power of GWAS using our
452 limited sample size. Nevertheless, this is the first report of QTLs for CHCs in any ant
453 species.

454 While neither the individual- nor the colony-level analyses identified the same locus as
455 being associated with more than one CHC, oftentimes QTLs of different CHCs were
456 found close by in the genome. It has been shown that some chromosomal regions form
457 distinct compartments in regards to their functionality and co-regulation[54,55]. We
458 hypothesize that the genomic clusters identified may be topological or functional
459 domains that are related to the synthesizing of CHCs. Insects synthesize hydrocarbons
460 by elongating fatty acyl-CoA precursors to produce long chain fatty acids that are then
461 converted to hydrocarbons[9]. The elongation reaction is responsible for regulating
462 hydrocarbons lengths[56] and thereby in determining the variation in quantities of various
463 CHCs with a range of chain lengths. Another source of variation is the addition of methyl

464 branches in different positions during the synthesis of the fatty acids. The candidate
465 QTLs may be related to these biosenthetic mechanisms, perhaps as polymorphic
466 regulatory factors. Further study of the candidate loci is needed in order to examine
467 their relation to CHC synthesis.

468 The ability to discriminate between nestmates and non-nestmates depends on the
469 differences between their CHC profiles[6,14–17]. We may expect that the more distinct their
470 colony CHC profile is, the easier it would be for nestmates to identify each other.
471 Colonies with rare genotypes in loci that regulate CHCs would therefore be favoured by
472 natural selection over colonies with common genotypes. Rare alleles would be selected
473 for so long they are rare, thus maintaining and increasing the polymorphism in the
474 population. Therefore, we may predict balancing (frequency-dependent) selection on
475 genes that regulate CHCs, in a similar fashion as in other recognition systems for which
476 polymorphism is advantageous for the discrimination of self vs. non-self, such as the
477 MHC immunity system in mammals[57,58] and the self-incompatibility system of plants[59].
478 This leads us to predict that CHC variation will increase in evolution through the
479 generation of polymorphic genetic loci that affect CHC synthesis and/or their secretion
480 on the cuticle, i.e. CHC QTLs.

481 Despite this prediction for the evolution of genetic polymorphism in nestmate
482 recognition cues, environmental factors may have greater contribution than genetic
483 factors to the phenotypic variation. In our analysis, only seven QTLs for four of the 34
484 CHCs were detected with a q-value < 0.05; two CHCs in the individual- and three in the
485 colony-level analysis (QTLs for CHC 5Me-C25 were detected in both analyses). Diet was

shown to influence the cuticular chemical profiles in the polygyne and polydomous colonies of *Formica aquilonia* ants, where nestmates are not necessarily related[19]. In comparison, the colonies of *C. niger* used in this study are monogyne[40], and so nestmates are always related (at least 25% relatedness). Environmental odours also appear to determine aggression levels between lab-reared and field-collected workers of monogyne *Solenopsis invicta* colonies[20] and similarly between lab-reared and field-collected polygyne *Rhytidoponera confusa* workers[18]. Considering the limited results from our GWAS, it appears that genetic factors have a lesser role than environmental factors in our study system.

Nevertheless, our analyses suggest that polymorphism in multiple genes contributes to CHC variation. The statistical power obtained from the sample size of 244 ants from 45 colonies limited our confidence in specific QTLs, yet we can conclude from the results that tens of QTLs affect CHCs. This observation is in line with studies in model insect species such as *Drosophila*, where larger sample sizes and more powerful experimental approaches are available. For example, a GWAS of CHCs conducted using 169 inbred lines from the *D. melanogaster* Genetic Reference Panel (DGRP) identified QTLs in 305 and 173 genes in females and males, respectively[60]. Also in *Drosophila*, it is likely that the sample size limits the statistical power of GWAS. The numbers of QTLs reported are likely underestimates because QTLs with smaller effect size are more difficult to detect. Therefore, we may conclude that CHCs have a complex polygenic genomic architecture, which is in line with their being complex quantitative traits.

507 The Gestalt model suggests that social interaction between colony members has an
508 important role in determining colony identity. Social interactions have substantial
509 impacts on many other phenotypes in insect societies. For example, when *Camponotus*
510 *floridanus* workers were fed with juvenile hormone, an important regulator of growth
511 and development in insects, the larvae they fed through trophallaxis were twice as likely
512 to become larger workers[61]. In termites, social interactions of allogrooming and
513 trophallaxis appear to contribute in determining the caste of developing brood[62]. The
514 physical transfer and mixing of CHCs between nestmates may be a major factor shaping
515 their chemical identity. In our colony-level analysis, transfer of CHCs between nestmates
516 is accounted for by the averaging out of nestmate genetics and their CHC phenotypes.
517 This analysis resulted in fewer QTLs identified in comparison to the individual-level
518 analysis, but in general with greater statistical significance, indicating more confidence
519 in the colony-level model. This result may be interpreted as supporting the Gestalt
520 model. Alternatively, it may be that the averaging of colonies' genotypes and
521 phenotypes helps in eliminating noise introduced in the chemical analysis and
522 sequencing/genotype errors, and so results in a more robust outcome. Additional
523 studies including behavioural analysis and manipulation may provide further insight into
524 the significance of the Gestalt model and determine the exact nature of social effects on
525 CHC profiles. Whichever is the case, our colony-level analysis was successful in revealing
526 putative QTLs, indicating that this approach is appropriate for CHCs. Whether the
527 Gestalt effect is present or not, genomic mapping of CHCs should be done at the colony
528 level due to the shared genetics and environment of nestmates.

Acknowledgements

We thank Abraham Hefetz for advice and access to equipment for chemical analysis of CHCs. We thank Jessica Purcell and Alan Brelsford for advice on RAD-seq. This study was funded by Israel Science Foundation grant number 646/15.

References

1. Hamilton, W. D. The genetical evolution of social behavior. I. *Gr. Sel.* 23–43 (1964).
2. Hamilton, W. D. Discrimination nepotism: expectable, common, overlooked. in *Kin Recognition in Animals ed* (ed. Michener, D. J. C. F. and C. D.) 417–437 (Wiley, 1987).
3. Errard, C. & Hefetz, A. Label familiarity and discriminatory ability of ants reared in mixed groups. *Insectes Soc.* **44**, 189–198 (1997).
4. Vernier, C. L. *et al.* The cuticular hydrocarbon profiles of honey bee workers develop via a socially-modulated innate process. *Elife* **8**, 1–27 (2019).
5. van Zweden, J. S. & D'Ettorre, P. Nestmate recognition in social insects and the role of hydrocarbons. *Insect Hydrocarb. Biol. Biochem. Chem. Ecol.* 222–243 (2010).
6. Lahav, S., Soroker, V., Hefetz, A. & Vander Meer, R. K. Direct behavioral evidence for hydrocarbons as ant recognition discriminators. *Naturwissenschaften* **86**, 246–249 (1999).
7. Dani, F. R. *et al.* Nestmate recognition cues in the honey Bee: Differential importance of cuticular alkanes and alkenes. *Chem. Senses* **30**, 477–489 (2005).
8. Hefetz, A. The evolution of hydrocarbon pheromone parsimony in ants (Hymenoptera: Formicidae) -- interplay of colony odor uniformity and odor idiosyncrasy. A review. *Myrmecol. News* **10**, 59–68 (2007).
9. Blomquist, G.J., Bagnères, A.-G. Insect Hydrocarbons: Biology, Biochemistry and Chemical Ecology. *Cambridge Univ.* (2010).
10. Martin, S. & Drijfhout, F. A review of ant cuticular hydrocarbons. *J. Chem. Ecol.* **35**, 1151–1161 (2009).
11. Howard, R. W. Chemical ecologyand biochemistry of insect hydrocarbons. *Annu. Rev. Entomol.* **27**, 149–172 (1982).
12. Howard, R. W. & Blomquist, G. J. Ecological, behavioral, and biochemical aspects of insect hydrocarbons. *Annu. Rev. Entomol.* **50**, 371–393 (2005).
13. Blomquist, G. J., Tittiger, C. & Jurenka, R. *Cuticular Hydrocarbons and Pheromones of Arthropods*. *Hydrocarbons, Oils and Lipids: Diversity, Origin, Chemistry and Fate* (2018).
14. Wagner, D., Tissot, M., Cuevas, W. & Gordon, D. M. Harvester ants utilize cuticular hydrocarbons in nestmate recognition. *J. Chem. Ecol.* **26**, 2245–2257 (2000).

563 15. Drescher, J., Blüthgen, N., Schmitt, T., Bühler, J. & Feldhaar, H. Societies drifting apart?
564 behavioural, genetic and chemical differentiation between supercolonies in the yellow
565 crazy ant anoplolepis gracilipes. *PLoS One* **5**, 1–8 (2010).

566 16. Foitzik, S., Sturm, H., Pusch, K., D'Ettorre, P. & Heinze, J. Nestmate recognition and
567 intraspecific chemical and genetic variation in Temnothorax ants. *Anim. Behav.* **73**, 999–
568 1007 (2007).

569 17. Blight, O. *et al.* Variation in the level of aggression, chemical and genetic distance among
570 three supercolonies of the Argentine ant in Europe. *Mol. Ecol.* **21**, 4106–4121 (2012).

571 18. Crosland, M. W. J. Kin recognition in the ant Rhytidoponera confusa II. Gestalt odour.
572 *Anim. Behav.* **37**, 920–926 (1989).

573 19. Sorvari, J., Theodora, P., Turillazzi, S., Hakkarainen, H. & Sundström, L. Food resources,
574 chemical signaling, and nest mate recognition in the ant Formica aquilonia. *Behav. Ecol.*
575 **19**, 441–447 (2008).

576 20. Obin, M. S. Nestmate recognition cues in laboratory and field colonies of Solenopsis
577 invicta buren (Hymenoptera: Formicidae) - Effect of environment and role of cuticular
578 hydrocarbons. *J. Chem. Ecol.* **12**, 1965–1975 (1986).

579 21. Sprenger, P. P. & Menzel, F. Cuticular hydrocarbons in ants (Hymeno ptera: Formicidae)
580 and other insects: how and why they differ among individuals, colonies, and species.
581 *Myrmecological News* **30**, 1026 (2020).

582 22. Teseo, S. *et al.* Genetic Distance and Age Affect the Cuticular Chemical Profiles of the
583 Clonal Ant Cerapachys biroi. *J. Chem. Ecol.* **40**, 429–438 (2014).

584 23. PROVOST, E. Nonnestmate kin recognition in the ant Leptothorax lichtensteini: evidence
585 that genetic factors regulate colony recognition. *Behav. Genet.* **21**, 151–167 (1991).

586 24. Van Zweden, J. S., Brask, J. B., Christensen, J. H., Boomsma, J. J. & Linksvayer, T. A.
587 D'ettorre, P. Blending of heritable recognition cues among ant nestmates creates distinct
588 colony gestalt odours but prevents within-colony nepotism. *J. Evol. Biol.* **23**, 1498–1508
589 (2010).

590 25. Crozier, R. H. & Dix, M. W. Analysis of two genetic models for the innate components of
591 colony odor in social Hymenoptera. *Behav. Ecol. Sociobiol.* **4**, 217–224 (1979).

592 26. Beye, M., Neumann, P. & Moritz, R. F. A. Nestmate recognition and the genetic gestalt in
593 the mound-building ant Formica polyctena. *Insectes Soc.* **44**, 49–58 (1997).

594 27. Beye, M., Neumann, P., Chapuisat, M., Pamilo, P. & Moritz, R. F. A. Nestmate recognition
595 and the genetic relatedness of nests in the ant Formica pratensis. *Behav. Ecol. Sociobiol.*
596 **43**, 67–72 (1998).

597 28. Soroker, V., Vienne, C., Hefetz, A. & Nowbahari, E. The postpharyngeal gland as a
598 'Gestalt' organ for nestmate recognition in the ant Cataglyphis niger. *Naturwissenschaften*
599 **81**, 510–513 (1994).

600 29. Dahbi, A. & Lenoir, A. Nest Separation and the Dynamics of the gestalt odor in the
601 polydomous ant Cataglyphis iberica (Hymenoptera , Formicidae). *Behav. Ecol.* **42**, 349–
602 355 (1998).

603 30. Crosland, M. W. J. Variation in ant aggression and kin discrimination ability within and
604 between colonies. *J. Insect Behav.* **3**, 359–379 (1990).

605 31. Ross, K. G. & Keller, L. Genetic control of social organization in an ant. *Proc. Natl. Acad.*
606 *Sci.* **95**, 14232–14237 (1998).

607 32. Beckers, R., Deneubourg, J. L. & Goss, S. Modulation of trail laying in the ant Lasius niger
608 (Hymenoptera: Formicidae) and its role in the collective selection of a food source. *J.*
609 *Insect Behav.* **6**, 751–759 (1993).

610 33. Sumpter, D. J. T. & Beekman, M. From nonlinearity to optimality: Pheromone trail
611 foraging by ants. *Anim. Behav.* **66**, 273–280 (2003).

612 34. Macevicz, S. & Oster, G. Modeling social insect populations II: Optimal reproductive
613 strategies in annual eusocial insect colonies. *Behav. Ecol. Sociobiol.* **1**, 265–282 (1976).

614 35. Huang, Y. C. & Wang, J. Did the fire ant supergene evolve selfishly or socially? *BioEssays*
615 **36**, 200–208 (2014).

616 36. Trivers, R. L. & Hare, H. Haplodiploidy and the evolution of the social insects. *Science*
617 **191**, 249–263 (1976).

618 37. Henri, J. F, R. J. What is an individual organism? A multilevel selection perspective. *Q.*
619 *Rev. Biol.* **85**, 1 (2010).

620 38. Inbar, S., Cohen, P., Yahav, T. & Privman, E. Comparative study of population genomic
621 approaches for mapping colony-level traits. *PLoS Comput. Biol.* **16**, (2020).

622 39. Eyer, P. A., Seltzer, R., Reiner-Brodetzki, T. & Hefetz, A. An integrative approach to
623 untangling species delimitation in the Cataglyphis bicolor desert ant complex in Israel.
624 *Mol. Phylogenet. Evol.* **115**, 128–139 (2017).

625 40. Brodetzki, T. R. *et al.* The Interplay between Incipient Species and Social Polymorphism in
626 the Desert Ant Cataglyphis. *Sci. Rep.* **9**, 9495 (2019).

627 41. Inbar, S. & Privman, E. The effect of chemical distances, physical distances, and the
628 presence of sexuals on aggression in Cataglyphis desert ants. *bioRxiv* (2018).

629 42. Bolger, A. M., Lohse, M. & Usadel, B. Trimmomatic: A flexible trimmer for Illumina
630 sequence data. *Bioinformatics* **30**, 2114–2120 (2014).

631 43. Langmead, B., Trapnell, C., Pop, M. & Salzberg, S. L. Ultrafast and memory-efficient
632 alignment of short DNA sequences to the human genome. *Genome Biol.* **10**, R25 (2009).

633 44. McKenna, Aaron, Matthew Hanna, Eric Banks, Andrey Sivachenko, Kristian Cibulskis,
634 Andrew Kernytsky, K. G. et al. The Genome Analysis Toolkit: A MapReduce framework for
635 analyzing next-generation DNA sequencing data. *Genome Res.* **20**, 1297– 1303 (2010).

636 45. Browning, B. L., Zhou, Y. & Browning, S. R. A One-Penny Imputed Genome from Next-
637 Generation Reference Panels. *Am. J. Hum. Genet.* **103**, 338–348 (2018).

638 46. Browning, B. L. & Browning, S. R. Improving the accuracy and efficiency of identity-by-
639 descent detection in population data. *Genetics* **194**, 459–471 (2013).

640 47. Peterson, B. K., Weber, J. N., Kay, E. H., Fisher, H. S. & Hoekstra, H. E. Double digest
641 RADseq: An inexpensive method for de novo SNP discovery and genotyping in model and
642 non-model species. *PLoS One* **7**, (2012).

643 48. Brelsford, A., Dufresnes, C. & Perrin, N. High-density sex-specific linkage maps of a
644 European tree frog (Hyla arborea) identify the sex chromosome without information on

645 offspring sex. *Heredity* 177–181 (2016) doi:10.1038/hdy.2015.83.

646 49. Catchen, J. M. Stacks: an analysis tool set for population genomics. *Mol. Ecol.* **22**, 3124–
647 3140 (2013).

648 50. Peterson RA, C. J. Ordered quantile normalization: a semiparametric transformation built
649 for the cross-validation era. *J. Appl. Stat.* 1–16 (2019).

650 51. Lipka, A. E. *et al.* GAPIT: Genome association and prediction integrated tool.
651 *Bioinformatics* **28**, 2397–2399 (2012).

652 52. Kang, H. M. *et al.* Variance component model to account for sample structure in genome-
653 wide association studies. *Nat. Genet.* **42**, 348–354 (2010).

654 53. Benjamini, Y. & Hochberg, Y. Controlling the False Discovery Rate : A Practical and
655 Powerful Approach to Multiple Testing. *J. R. Stat. Soc.* **57**, 289–300 (1995).

656 54. Goetze, S. *et al.* The Three-Dimensional Structure of Human Interphase Chromosomes Is
657 Related to the Transcriptome Map. *Mol. Cell. Biol.* **27**, 4475–4487 (2007).

658 55. Matharu, N. K. & Ahanger, S. H. Chromatin insulators and topological domains: Adding
659 new dimensions to 3D genome architecture. *Genes.* **6**, 790–811 (2015).

660 56. Blomquist, G. J., Vogt, R. G. *Insect Pheromone Biochemistry and Molecular Biology*.
661 (Elsevier Academic Press, 2003).

662 57. Hedrick, P. W. Balancing selection and MHC. *Genetica* **104**, 207–214 (1998).

663 58. Aguilar, A. *et al.* High MHC diversity maintained by balancing selection in an otherwise
664 genetically monomorphic mammal. *Proc. Natl. Acad. Sci. U. S. A.* **101**, 3490–3494
665 (2004).

666 59. Glémin, S. *et al.* Balancing selection in the wild: Testing population genetics theory of
667 self-incompatibility in the rare species Brassica insularis. *Genetics* **171**, 279–289 (2005).

668 60. Dembeck, L. M. *et al.* Genetic architecture of natural variation in cuticular hydrocarbon
669 composition in Drosophila melanogaster. *Elife* **4**, (2015).

670 61. LeBoeuf, A. C. *et al.* Oral transfer of chemical cues, growth proteins and hormones in
671 social insects. *Elife* **8**, (2016).

672 62. Watanabe, D., Gotoh, H., Miura, T. & Maekawa, K. Social interactions affecting caste
673 development through physiological actions in termites. *Front. Physiol.* **5**, 1–12 (2014).

674

675 # Data Accessibility

676 Genomic sequencing data will be made public upon acceptance of the paper in the NCBI SRA database.
677 Chemical data will be made public in the Dryad repository.

Supplementary materials

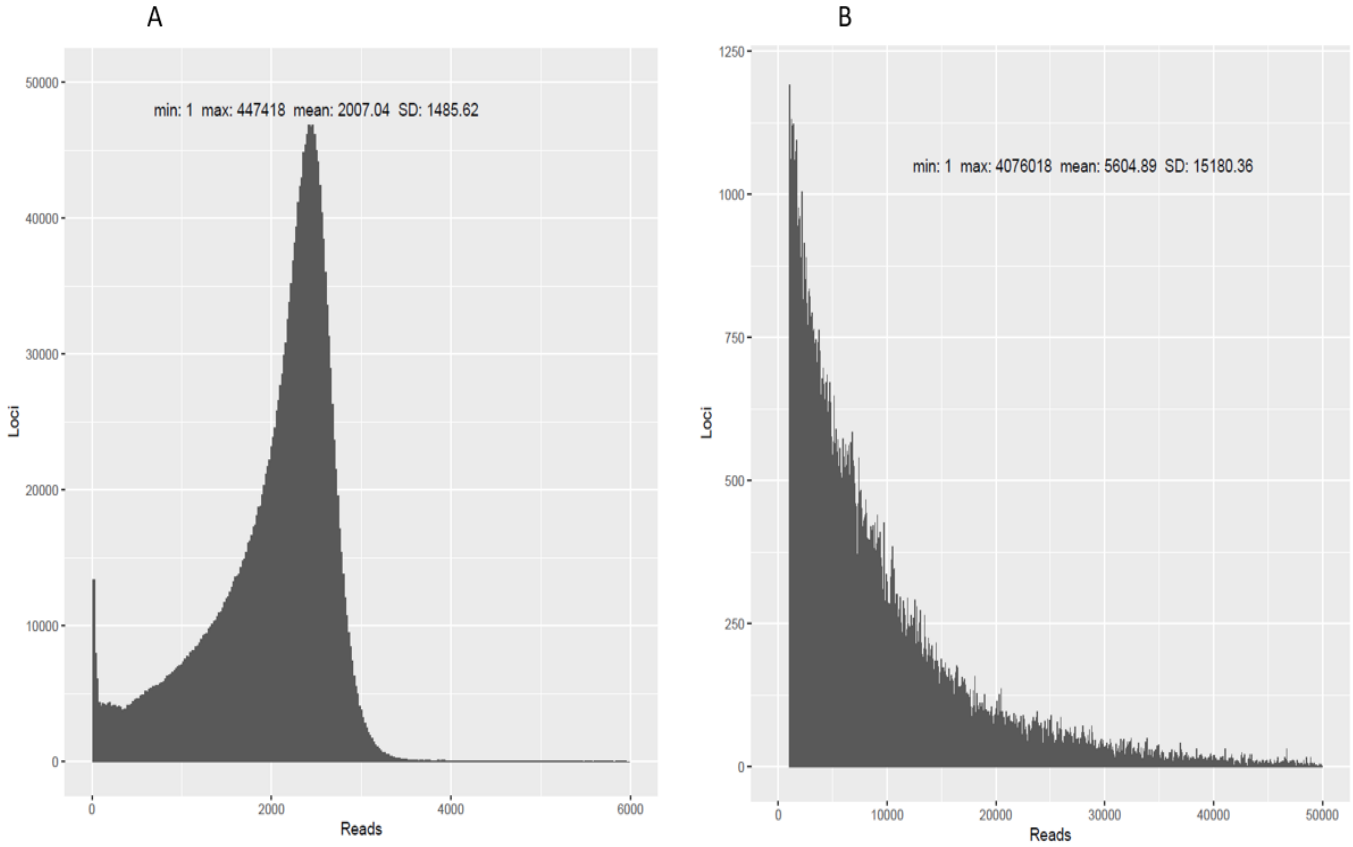

Figure S1. Distribution and summary statistics of the number of reads across unfiltered loci. (A) 276 fully sequenced samples from 47 colonies sampled in Betzet beach in northern Israel. (B) 47 RAD-sequenced samples of 47 colonies from which the fully sequenced samples also originate.

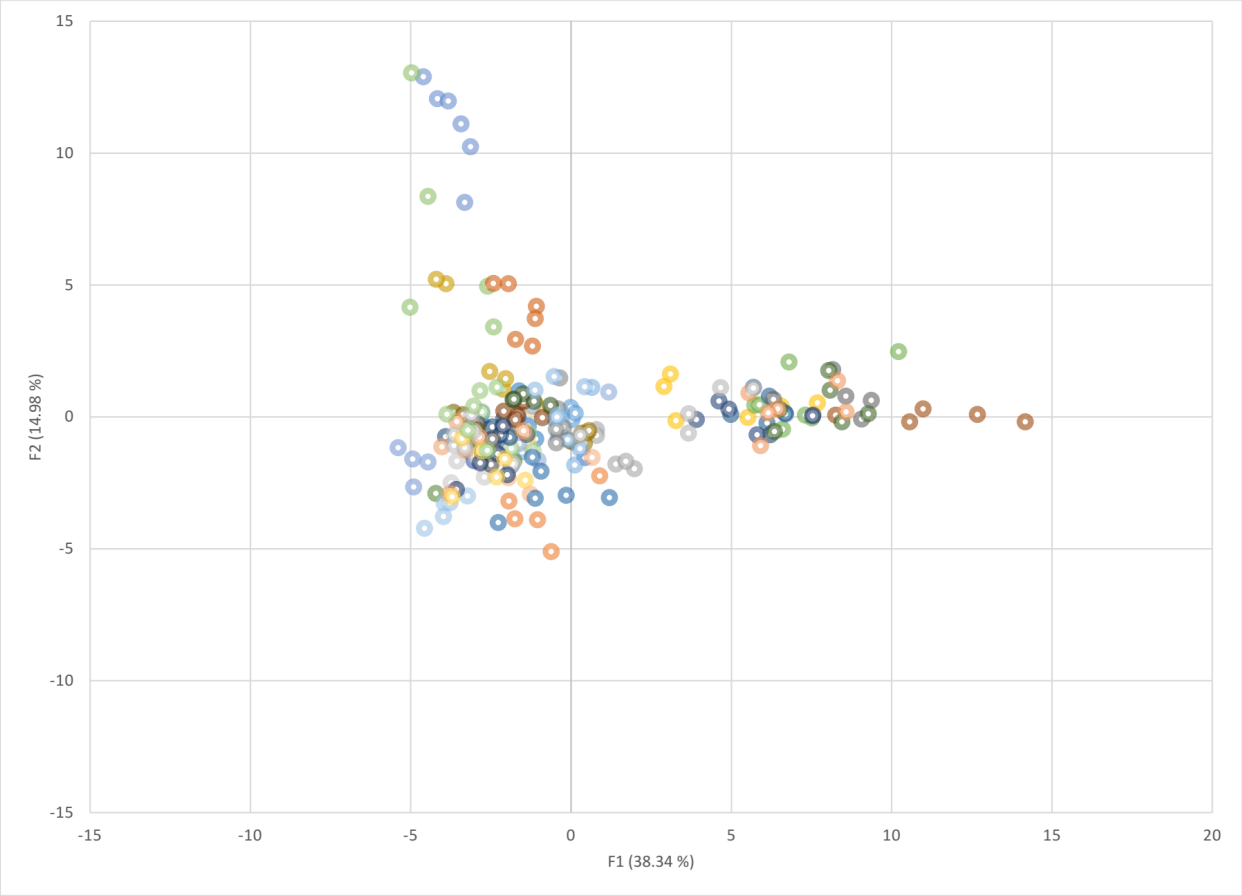

683

684 **Figure S2**. Discriminant analysis (DA) of the chemical signature of all colonies examined in this
685 study. Samples from different nests are marked by different colors. Wilks' Lambda test (Rao's
686 approximation) indicate a statistical difference between colonies (p-value<0.0001).

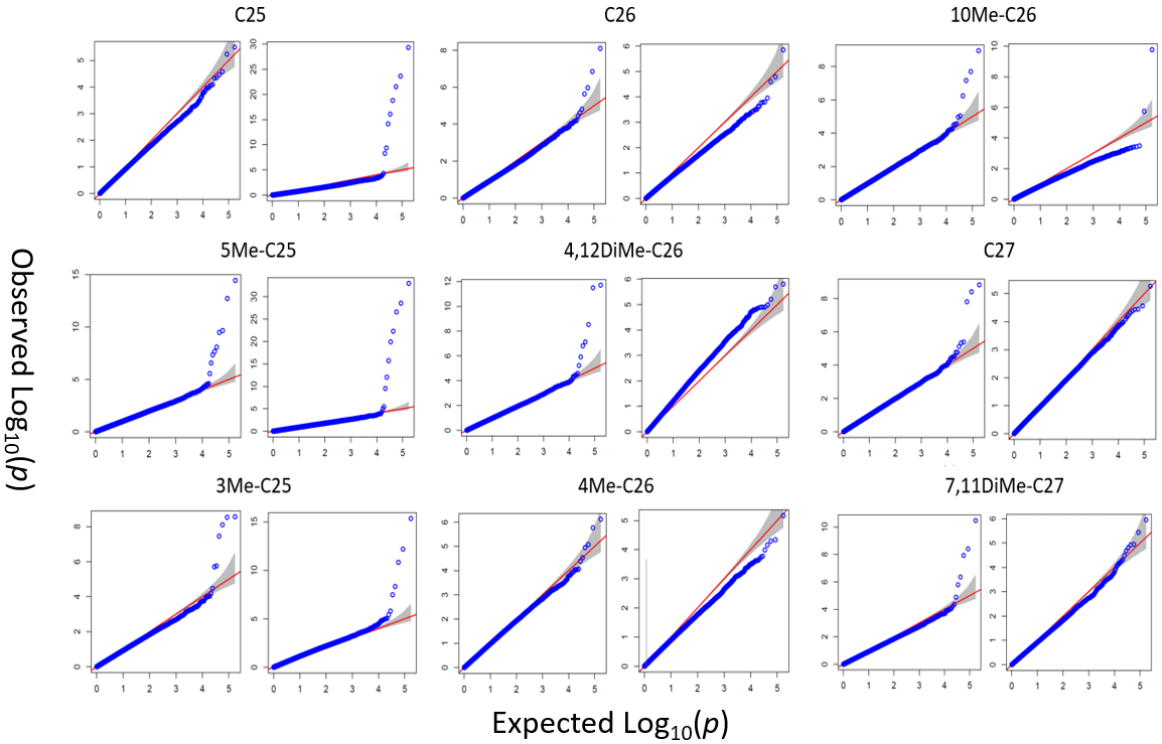
C25
C26
10Me-C26
5Me-C25
4,12DiMe-C26
C27
3Me-C25
4Me-C26
7,11DiMe-C27
Observed Log10(p)
Expected Log10(p)

687

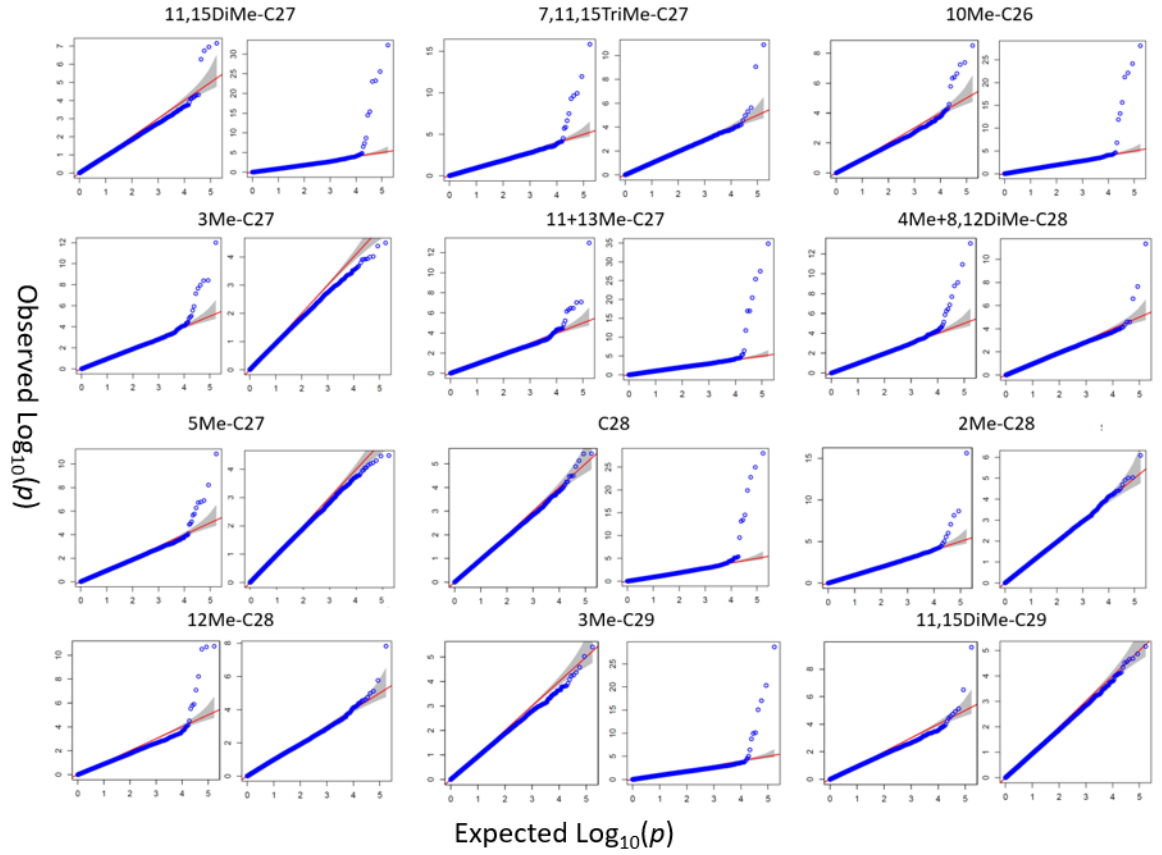
11,15DiMe-C27
7,11,15TriMe-C27
10Me-C26
3Me-C27
11+13Me-C27
4Me+8,12DiMe-C28
5Me-C27
C28
2Me-C28
12Me-C28
3Me-C29
11,15DiMe-C29
Observed Log10(p)
Expected Log10(p)

688

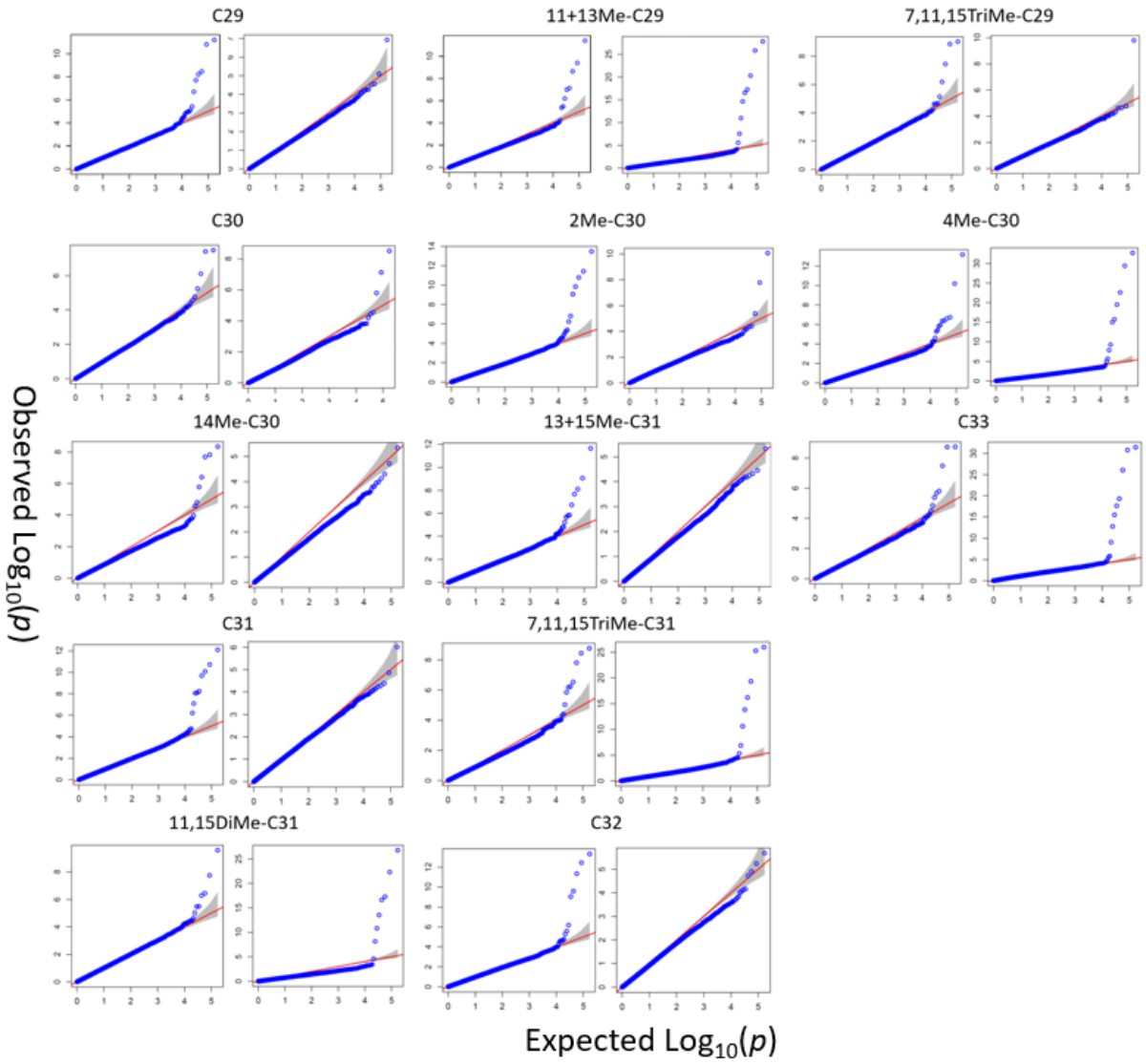

Figure S3. Assesment of how well the model used in the inidivual-level (left) and colony-level (right) analyses accounts for familial relatedness and population strcture for each of the CHC traits. The negative logarithms of the loci *p*-values S are plotted against their expected value under the null hypothesis of no association with the trait.

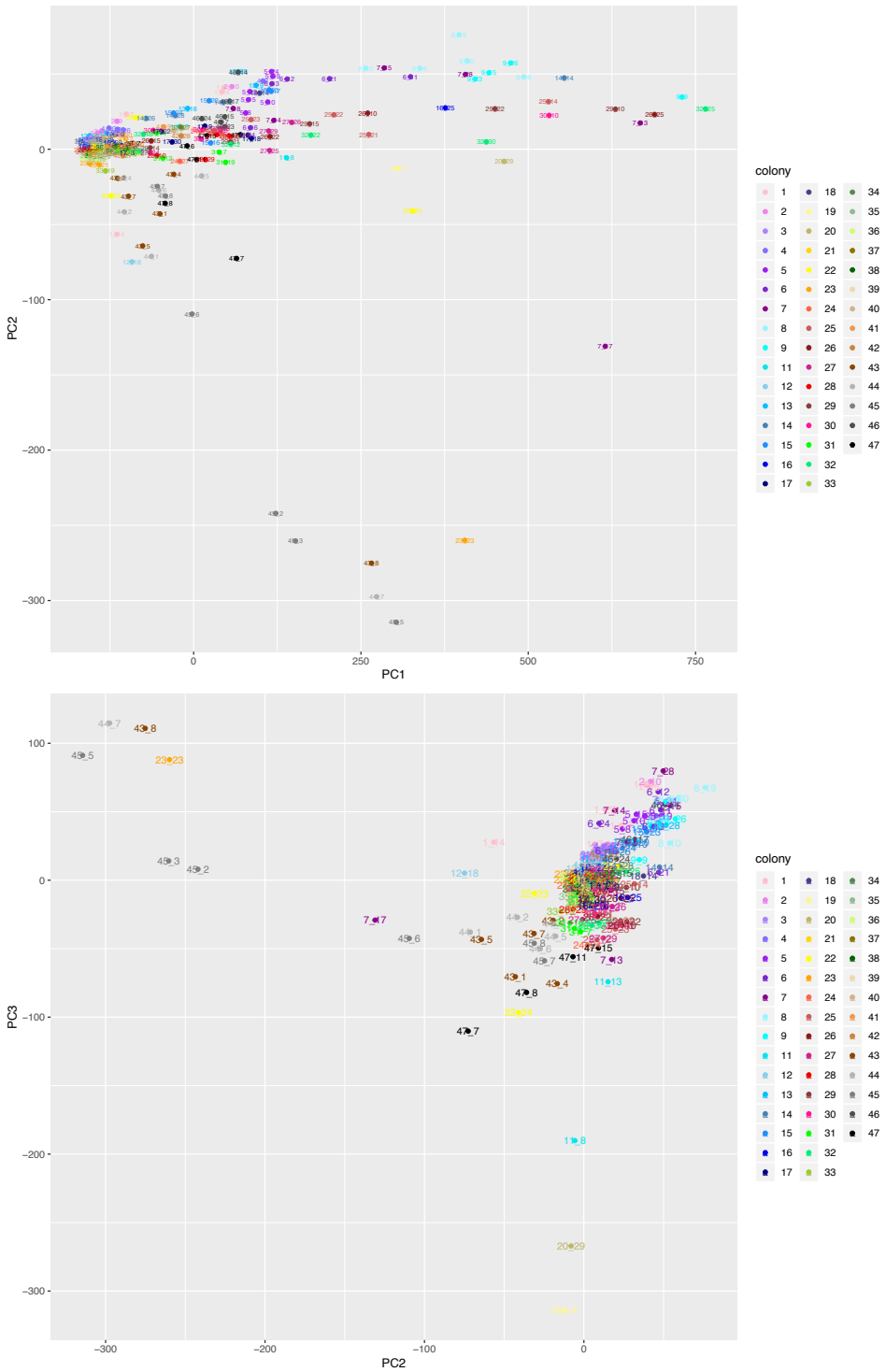

Figure S4. Principle Component Analysis (PCA) of genotype data from 244 individuals of 45 colonies colored by colony ID. Note that colonies were numbered from north to south along the transect.

A

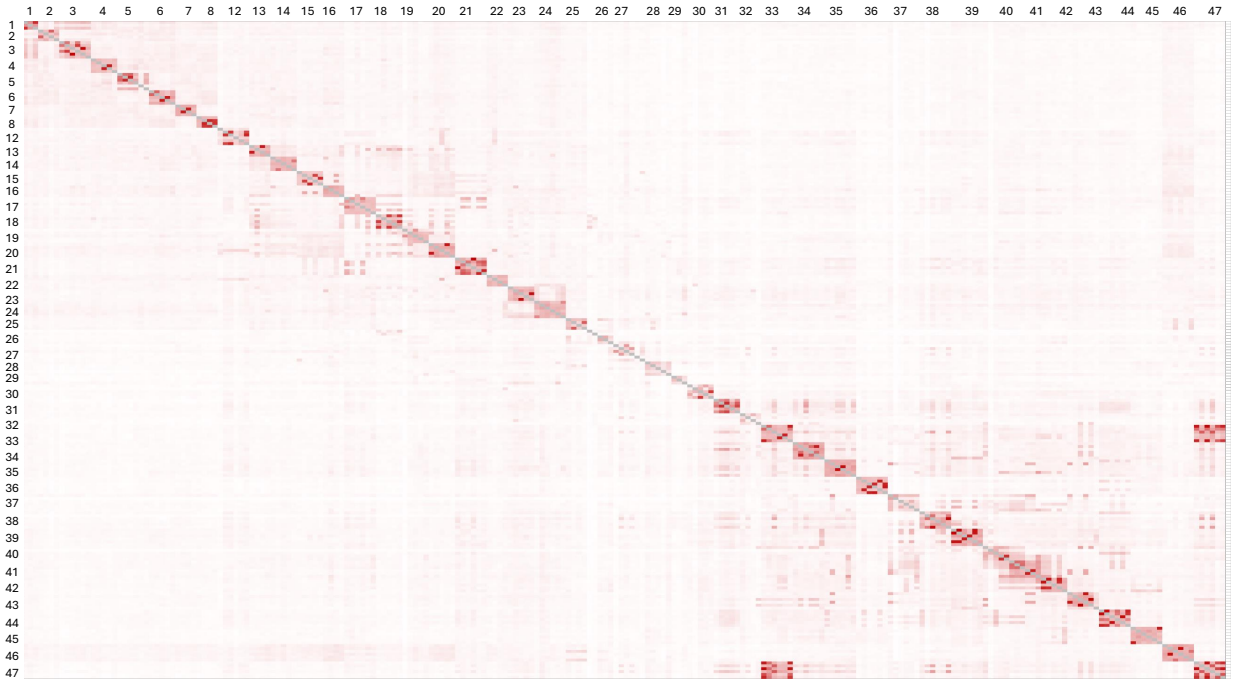

B

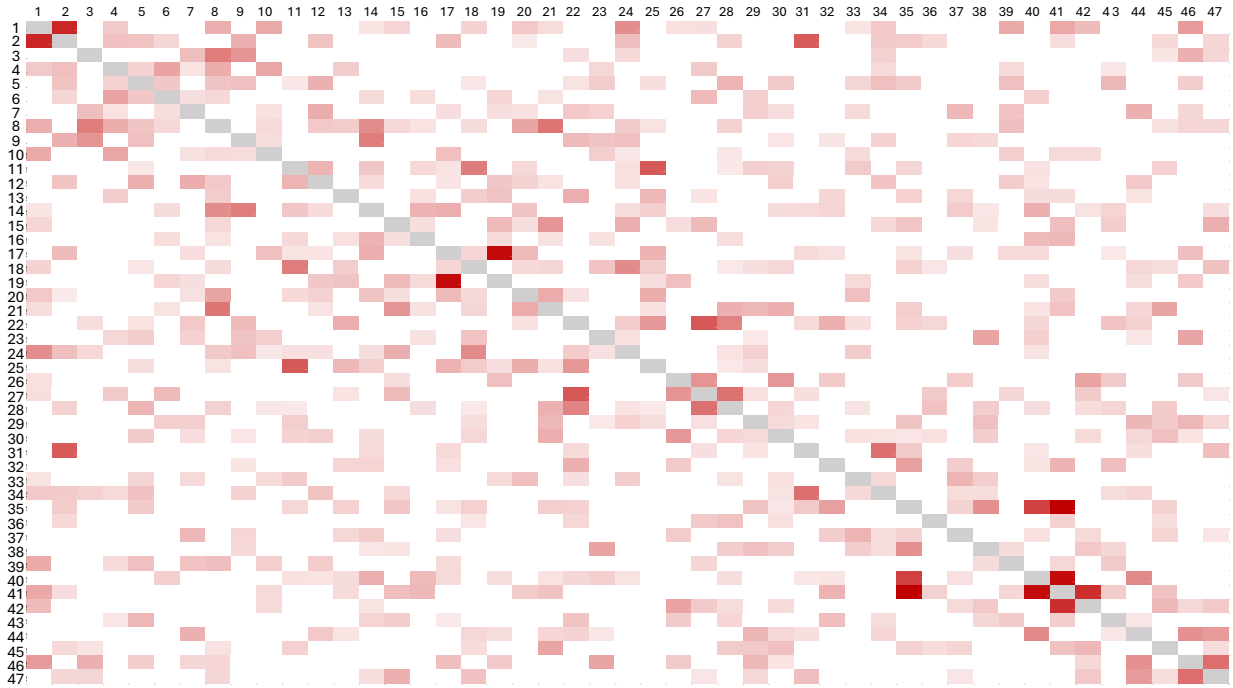

Figure S5. Kinship matrices based on the total length of shared IBD haplotypes between 244 individuals of 45 colonies (A) and 47 individuals of 47 colonies (B). For visibility, only colony numbers are presented. The heatmap coloring is based on the total number of bases in shared haplotypes between each pair of samples. Higher values are stronger red.

709 **Table S1**. Outlayer removals and normalization methods of the phenotype on the individual and
710 colony level.

Trait	Individual-level outlayers	Individual-level normalization	Colony-level outlayers	Colony-level normalization
C25	17	Yeo-Johnson	0	Log_b(x + a)
5Me-C25	44	Order norm	9	Log_b(x + a)
3Me-C25	22	Log_b(x + a)	4	Box Cox
C26	23	sqrt(x + a)	2	Box Cox
10Me-C26	13	Log_b(x + a)	2	sqrt(x + a)
4Me-C26	20	Order norm	3	Log_b(x + a)
4,12DiMe-C26	12	asinh(x)	1	sqrt(x + a)
C27	11	Order norm	2	Log_b(x + a)
5Me-C257	5	asinh(x)	0	sqrt(x + a)
11+13Me-C27	13	Order norm	2	Log_b(x + a)
11,15DiMe-C27	37	Order norm	9	Log_b(x + a)
7,11DiMe-C27	2	Yeo-Johnson	0	asinh(x)
3Me-C27	16	Box Cox	1	Box Cox
7,11,15TriMe-C27	21	exp(x)	4	asinh(x)
C28	37	Order norm	4	sqrt(x + a)
12Me-C28	13	Order norm	0	asinh(x)
4,12DiMe-C28	1	Box Cox	0	sqrt(x + a)
4Me+8,12DiMe-C28	16	sqrt(x + a)	0	Box Cox
2Me-C28	23	Order norm	2	sqrt(x + a)
C29	14	Box Cox	1	sqrt(x + a)
11+13Me-C29	13	Box Cox	1	Box Cox
11,15DiMe-C29	17	Yeo-Johnson	2	Log_b(x + a)
3Me-C29	34	Order norm	3	sqrt(x + a)
7,11,15TriMe-C29	5	Box Cox	3	sqrt(x + a)
C30	26	Yeo-Johnson	4	asinh(x)
14Me-C30	15	Box Cox	2	asinh(x)
4Me-C30	16	Order norm	0	Log_b(x + a)
2Me-C30	14	asinh(x)	4	Log_b(x + a)
C31	14	Log_b(x + a)	3	Box Cox
13+15Me-C31	11	exp(x)	4	sqrt(x + a)
11,15DiMe-C31	11	Box Cox	0	Log_b(x + a)
7,11,15TriMe-C31	4	Box Cox	0	asinh(x)
C32	13	asinh(x)	4	asinh(x)
C33	8	asinh(x)	0	sqrt(x + a)

711

712

Table S2. The mapping of significant loci (*q*-value < 0.3) on the genome. Individual-level GWAS results are in blue and colony-level GWAS results are in black**.** Loci that are mapped to the same or close genetic position (within 12cM) are marked with yellow or orange backgrounds. Both genetic and physical positioning are shown.

Chrom	Genetic pos (cM)	Scaffold	Position	CHC	q-value
1	0	scaffold17|size760598	515848	4,12DiMe-C26	0.279715055
1	2.87	scaffold35|size591243	473891	4,12DiMe-C26	0.11352072
1	9.66	scaffold296|size210905	44019	4,12DiMe-C26	0.279715055
1	34.15	scaffold578|size105271	38187	7,11,15TriMe-C27	0.168010666
1	88.15	scaffold916|size58012	4774	C31	0.118061549
1	88.15	scaffold293|size211391	198932	C33	0.281531387
2	65.4	scaffold636|size94593	82725	3Me-C25	0.281531387
3	85.67	scaffold320|size199217	33276	11+13Me-C27	0.259138689
3	87.52	scaffold1113|size42492	15042	4Me+8,12DiMe-C28	0.168010666
4	1.88	scaffold1163|size40329	39019	4Me+8,12DiMe-C28	0.201612799
4	16.6	scaffold558|size111151	58293	11+13Me-C29	0.145481369
4	39.56	scaffold77|size466230	39015	4,12DiMe-C26	0.23006866
4	39.56	scaffold551|size113931	79453	C31	0.144009142
4	83.57	scaffold326|size196711	73375	11+13Me-C27	0.009092586
4	143.72	scaffold220|size265453	70637	C32	0.163469837
4	181.71	scaffold734|size79827	17289	7,11,15TriMe-C27	0.23793943
4	203.11	scaffold74|size472645	164044	C31	0.118061549
5	131.68	scaffold35|size591243	43412	5Me-C25	0.106385132
6	70.38	scaffold336|size190304	25911	C29m3	0.181851711
6	90.66	scaffold737|size79726	15861	C28	0.251561534
7	52.75	scaffold107|size407829	186705	C33	0.281531387
7	56.43	scaffold859|size63718	3120	7,11,15TriMe-C27	0.168010666
7	57.35	scaffold19|size722566	429439	C31	0.144009142
7	62.08	scaffold279|size219011	173386	11,15DiMe-C27	0.018185171
7	101.52	scaffold30|size631625	144566	C28	0.275375449
7	104.36	scaffold85|size450463	361438	11+13Me-C29	0.175789988
7	111.1	scaffold28|size641708	145558	4Me+8,12DiMe-C28	0.21114854
7	135.68	scaffold404|size159223	63505	3Me-C25	0.281531387
8	126.41	scaffold194|size285062	81296	11+13Me-C29	0.175789988
8	137.97	scaffold618|size98603	6938	C31	0.118061549
8	208.22	scaffold658|size91109	44118	11,15DiMe-C27	0.297782177
8	222.43	scaffold740|size79674	67018	C32	0.096871015
8	259.2	scaffold20|size721085	484650	C29	0.28516405
8	309.3	scaffold751|size78167	6597	7,11,15TriMe-C29	0.287585825
9	45.61	scaffold54|size511285	140799	5Me-C25	0.009092586
9	85.74	scaffold235|size251712	52728	C32	0.090816576
9	119.36	scaffold219|size265940	180069	7,11,15TriMe-C27	0.168010666
9	137.13	scaffold311|size203550	120617	C29	0.186173981
9	142.85	scaffold505|size124814	43537	12Me-C28	0.093843796
9	142.85	scaffold66|size491290	166504	4Me+8,12DiMe-C28	0.276082392
10	105.07	scaffold306|size205911	65549	12Me-C28	0.093843796

10	132.88	scaffold75|size469975	364802	4Me+8,12DiMe-C28	0.21114854
11	2.02	scaffold146|size337763	226678	7,11,15TriMe-C27	0.271314522
11	17.44	scaffold291|size213446	9721	4Me-C30	0.099898234
11	44.83	scaffold22|size714790	90604	11+13Me-C27	0.275808429
11	111.65	scaffold67|size489733	28054	C31	0.189579603
11	153.29	scaffold622|size97615	36744	3Me-C25	0.292883459
11	312.17	scaffold508|size123518	117137	12Me-C28	0.093843796
12	0	scaffold730|size80008	50311	2Me-C30	0.240663927
12	67.25	scaffold71|size482159	21063	4Me+8,12DiMe-C28	0.21114854
12	77.84	scaffold71|size482159	252805	4Me+8,12DiMe-C28	0.215941637
12	87.97	scaffold593|size103847	95748	11+13Me-C29	0.19614006
12	94.99	scaffold65|size491780	101529	7,11,15TriMe-C27	0.271314522
12	115.45	scaffold209|size272198	146941	5Me-C25	0.045408288
12	141.58	scaffold470|size137511	24197	C31	0.226032368
14	40.37	scaffold44|size549762	519588	11+13Me-C29	0.175789988
14	48.21	scaffold581|size104792	64268	5Me-C25	0.207830527
14	50.17	scaffold125|size365959	224995	7,11,15TriMe-C29	0.254286414
14	92.55	scaffold204|size276989	165280	4Me+8,12DiMe-C28	0.072653261
14	95.38	scaffold144|size340398	186437	5Me-C25	0.141844335
14	107.79	scaffold3|size1157121	1010964	2Me-C30	0.265638486
14	127.94	scaffold130|size360227	149410	4Me+8,12DiMe-C28	0.168010666
15	52.68	scaffold72|size474807	247511	4,12DiMe-C26	0.11352072
15	90.15	scaffold124|size367063	14584	5Me-C25	0.093086991
15	94.21	scaffold99|size421651	410341	5Me-C25	0.027244973
15	174.71	scaffold212|size271006	160026	11+13Me-C27	0.172551495
16	40.47	scaffold1|size1555347	1092532	11,15DiMe-C27	0.297782177
17	55.6	scaffold299|size209978	118401	C31	0.118061549
17	68.45	scaffold29|size639771	423039	5Me-C25	0.072740685
17	147.15	scaffold608|size100611	57366	7,11,15TriMe-C27	0.018163315
18	74.77	scaffold153|size330014	258009	12Me-C28	0.220230198
18	117.35	scaffold61|size494520	99800	11+13Me-C29	0.175789988
18	136.63	scaffold13|size775888	175137	5Me-C25	0.141844335
18	148.94	scaffold74|size472645	467205	C28	0.227314639
20	0	scaffold1423|size26545	12315	5Me-C25	0.181851711
20	83.75	scaffold53|size513719	234805	4Me+8,12DiMe-C28	0.108979892
20	110.88	scaffold392|size162570	49495	5Me-C25	0.045462928
21	56.5	scaffold52|size514423	369128	7,11,15TriMe-C29	0.254286414
22	85.98	scaffold271|size223719	127531	C28	0.24549981
23	19.07	scaffold16|size761867	381681	3Me-C25	0.281531387
23	45.16	scaffold180|size296944	252701	C29	0.28516405
23	252.96	scaffold588|size104489	7055	C29	0.28516405
23	278.7	scaffold583|size104635	55219	C28	0.275375449
23	346.55	scaffold27|size651064	287045	C32	0.174367827
23	347.46	scaffold113|size393933	273321	2Me-C30	0.118061549
23	370.92	scaffold232|size254158	2527	5Me-C25	0.106385132
24	143.62	scaffold323|size197691	182834	2Me-C30	0.265638486
24	189.98	scaffold628|size95885	66061	C29	0.186173981

24	243.79	scaffold215|size268708	257542	11+13Me-C29	0.232997505
24	284.75	scaffold26|size661983	198368	5Me-C25	0.106385132
25	67.31	scaffold6|size960371	700278	C32	0.090816576
25	84.71	scaffold155|size327501	273726	C31	0.144009142
25	94.57	scaffold19|size722566	309358	C28	0.261411835
26	21.23	scaffold553|size113576	90729	11,15DiMe-C27	0.297782177
26	33.21	scaffold33|size606826	197846	12Me-C28	0.292429376
26	127.17	scaffold804|size70630	40423	5Me-C25	0.093086991
26	221.23	scaffold57|size507111	381549	C28	0.275375449
26	278.97	scaffold303|size207491	10542	11+13Me-C29	0.145481369
26	309.97	scaffold8|size894206	191498	7,11,15TriMe-C27	0.264881681